Hindawi
Journal of Nanomaterials
Volume 2018, Article ID 8632350, 10 pages
https://doi.org/10.1155/2018/8632350

Research Article

Effects of Biceramic AlN-SiC Microparticles on the Thermal Properties of Paraffin for Thermal Energy Storage

Arash Badakhsh,[1,2] Kay-Hyeok An,[3] Chan Woo Park,[2] and Byung-Joo Kim[1]

[1]*Research Laboratory for Multifunctional Carbon Materials, Korea Institute of Carbon Convergence Technology (KCTECH), Jeonju, Jeonbuk 54853, Republic of Korea*
[2]*Department of Mechanical Design Engineering, Chonbuk National University, Jeonju, Jeonbuk 54896, Republic of Korea*
[3]*Department of Carbon and Nano Materials Engineering, Jeonju University, Jeonju 55069, Republic of Korea*

Correspondence should be addressed to Kay-Hyeok An; khandragon@jj.ac.kr, Chan Woo Park; cw-park@jbnu.ac.kr, and Byung-Joo Kim; kimbj2015@gmail.com

Received 23 March 2018; Accepted 28 May 2018; Published 6 September 2018

Academic Editor: Yichen Guo

Herein, simplified time-efficient production of AlN-coated SiC (SiC@AlN) ceramic powder was practiced. Short-term vibratory ball milling with high frequency was employed to integrate the microsize particles. Also, paraffin as a significant phase change material (PCM) was reinforced using the manufactured SiC@AlN in order to enhance the thermal conductivity (TC) and stability of the final composite. Various characterization methods were used to clarify the changes in particle size of the biceramic powder as well as the thermal features of the paraffin-based composite. Manufactured SiC@AlN was found to be the most effective in the improvement of interfacial adhesion of composite components and the subsequent enhancement of TC, compared with singular ceramic powders as the reinforcing agents. Also, differential scanning calorimetry (DSC) indicated a very slight increase in latent heat of the fabricated composite PCM.

1. Introduction

Energy can be stored in different forms via a variety of methods. Among these, storage of energy utilizing the latent heat thermal storage (LHTS) and phase change is of interest owing to its simplicity and efficiency and to the abundance of such forms of wasted energy in large quantities. Several characteristics of paraffin wax including suitable melting point, large latent heat (145–240 kJ/kg), chemical stability with regular degradation level, process adaptability, low cost, and low environmental effects present this material as a promising phase change material (PCM) for LHTS purposes. However, engineers still face a significant challenge dealing with paraffin, specifically its intrinsic low thermal conductivity (i.e., below 0.4 W/m·K). To tackle such difficulty and further improve the desired responses in energy storage such as melting/solidification onset temperatures, durability, and chemical inertness, additives have been used to produce a paraffin-based composite PCM [1–7].

Due to their substantially high melting point, chemical stability and durability, and significant high-temperature tolerability, ceramics could also be used as efficient media for energy storage. Dhaidan et al. [8] used CuO for paraffin reinforcement and performed experimental and numerical investigations on the melting behaviour of the resultant composite PCM. Ho and Gao [9] reported the changes in the values of thermal conductivity and effective dynamic viscosity for the paraffin-based PCM loaded with 0, 5, and 10 wt.% of Al_2O_3 as the reinforcing agent. As a result, a rather nonlinear dependence of the thermal conductivity and the effective dynamic viscosity of the PCM on the mass fraction of Al_2O_3 was observed. A maximum increase in thermal conductivity was reported to be 17% by using 10 wt.% of Al_2O_3 measured at 60°C. A comparison between Al_2O_3 and CuO was numerically studied by Valan Arasu et al. [10] on the thermal performance enhancement of paraffin wax. They reported a marginal enhancement with both fillers, where the melting and solidification behaviour of Al_2O_3@paraffin

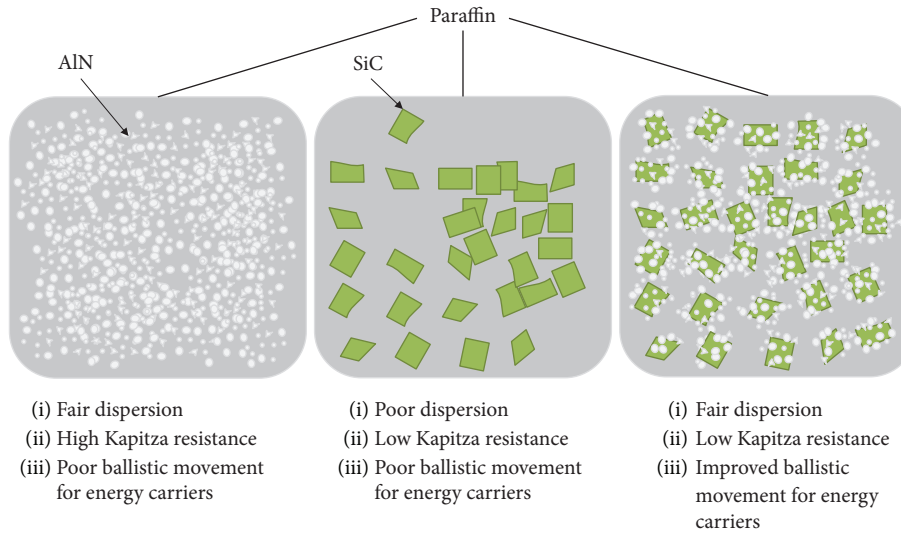

Figure 1: Schematic illustration of the formation of the better filler-matrix interface and better pathways for heat conduction in SiC@AlN powder.

was better due to the lower growth in dynamic viscosity compared to the use of CuO as a filler with the same mass fraction. Teng and Yu [11] experimentally studied the effect of different ceramic additives (Al_2O_3, TiO_2, SiO_2, and ZnO) on the LHTS performance of paraffin wax. They concluded that TiO_2 exhibits a better enhancement in thermal energy storage performance as it increases the thermal conduction and solidification onset temperature while reducing the melting onset temperature of paraffin. In the present study, a new series of ceramic fillers were employed to enhance the thermal energy storage behaviour of paraffin. Because of their low density, low thermal expansion, considerably high thermal conductivity, superior thermal shock resistance, and relatively low cost, aluminium nitride (AlN) [12] and silicon carbide (SiC) were selected as the target ceramic fillers. Interface enhancement is the most significant issue in fabrication of composites. Recently, a rather new trend of multiple-filler composite systems has emerged which is aimed at surface enhancement of components to achieve better interactions between the filler and the matrix [13–17]. Herein, to facilitate the encapsulation of SiC particles and subsequent formation of passages for heat conduction within the matrix, a considerable gap was selected between the average sizes of particles for the two ceramic components. The objective is to enhance the adhesion of the paraffin wax to the powder (see Figure 1). For this purpose, production of AlN-coated SiC (SiC@AlN) via time-efficient high-energy ball milling was practiced to unveil the effect of biceramic blend as well as of the singular fillers on the thermal performance of the resultant PCMs. A variety of characterization methods were carried out to thoroughly investigate the fillers and thermal features of the final composite PCMs.

2. Materials and Methods

2.1. Materials. Paraffin wax, aluminium nitride (powder, ≥98%), and silicon carbide (powder, 200–450 meshes) were all purchased from Sigma-Aldrich Chemicals Company, United States. All of the mentioned materials were used without any further purification. Some of the physical and thermophysical specifications of as-received materials are shown in Table 1.

2.2. Powder Preparation. The mechanical alloying method via vibratory mini ball mill (Pulverisette 23, Fritsch International, Germany) was used in order to mechanically fuse the AlN on the surface of SiC particles and enhance the particle bonding in the biceramic powder. Also, it likely facilitates the production of a uniformly distributed particle size within the functionally coated SiC, where AlN and SiC particles are 6 and 67.8 μm in diameter, respectively. Accordingly, SiC@AlN powder is expected to enhance the thermal energy storage capacity of paraffin while maintaining the intrinsic low electrical conductivity of the matrix as it could be potentially used as phase change thermal energy storage medium.

Different variables have been considered to optimize the integration and uniformity of the final SiC@AlN powder. 15, 30, and 50 Hz were chosen as the studied milling frequencies, where the milling time and ball-to-powder mass ratio (BPR) vary from 15 to 120 min and 4 : 1 to 20 : 1, respectively. The mass fraction of each component in the biceramic powder was kept constant at 50 wt.%. The grinding ball (15 mm in diameter) and the milling vial (10 ml) were both made of zirconia (95% ZrO_2).

For single-filler systems, AlN particles were used as received and pristine (as-received) SiC particles were exposed to the mechanical stress via ball milling for 60 min at 50 Hz to minimize the deposition of powder while moulding and enhance the dispersion of SiC within the matrix. Ball-milled SiC with an average particle diameter of about 28.53 μm will be referred to as "SiC" throughout this report unless otherwise mentioned.

2.3. Composite PCM Preparation. Uniformly mixing the composed biceramic powder with the liquefied paraffin is the next step in the PCM fabrication. A rather simple, but

Table 1: Specifications of as-received materials.

Material	Average particle size (μm)	ρ (g/cm^3) at 25°C [18]	k (W/m·K) at 25°C	C_p (J/kg·K) at 0–100°C	Melting point (°C) [18]
Paraffin wax	—	0.90	<0.4 [19]	2140–2900 [20]	53–57 (ASTM D87)
Aluminium nitride (AlN)	6.0	3.26	320 [21]	819.7 [22]	>2200
Silicon carbide (SiC)	67.8	3.22	270 [21]	675.4 [23]	2700

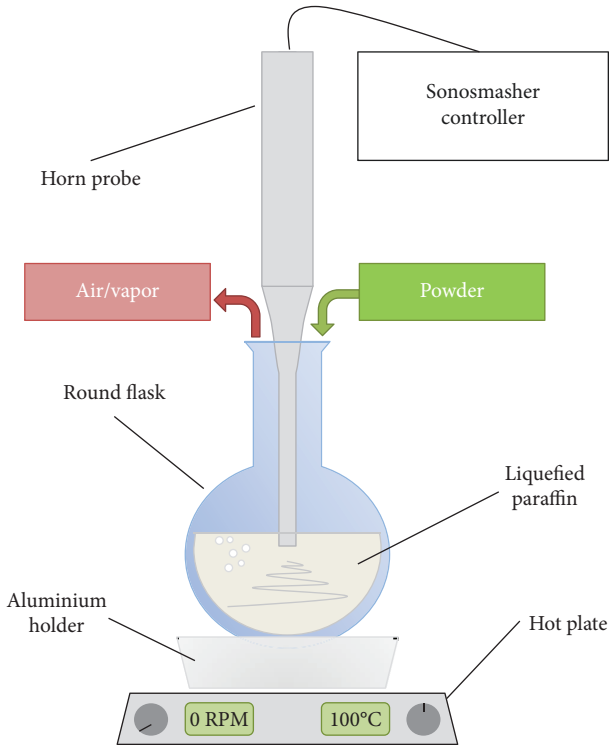

Figure 2: Graphic illustration of the mixing process.

effective, method was used employing an ultrasonic generator (Sonosmasher, Ulsso Hitech Co. Ltd., Korea) to increase the dispersion of the solid particles within the melted paraffin wax while reducing the number of trapped bubbles and gaseous impurities in the mixture. This process is graphically shown in Figure 2. During the sonication process, the mixture was regularly monitored to ensure the minimum deposition of the powder by controlling the input power of the ultrasonic generator (10–30%). The hot plate was kept at 100°C, and the mass fraction ratio of the filler to the whole composite PCM is 5 wt.% for all the cases.

3. Results and Discussion

3.1. Particle Morphology. SEM images of the as-received and as-prepared particles are shown in Figure 3. As seen here, AlN particles are physically attached to the surface of the deformed SiC.

3.2. Particle Size Analysis. A step-by-step procedure via a laser diffraction particle size analyzer (Microtrac S3500 integrated with a wet SDC unit, Microtrac Inc., United States) was carried out to individually optimize each parameter leading to the final set of optimum variables. Firstly, the effect of different milling frequencies (15, 30, and 50 Hz) with variations in BPR on the particle size distribution (PSD) was examined, while the ball milling time was kept constant at 15 min. The PSD graphs are illustrated in Figure 4 with respect to changes in the milling frequency. As the ball milling frequency increases, the particle diameter tends to decrease, specifically a dramatic reduction in the highest peak, due to the impact force and shear stress between the particles, ball, and walls of the milling vial. It also indicates that the particle size integration in SiC@AlN powder is possible as multipeak graphs are inclined to unify in a single-peak curve with the increase in frequency. Therefore, the mechanical stress when the milling frequency is at 50 Hz tends to alloy the AlN on SiC particles noting that fracture effects are also at minimum due to the large gap of about 11 times between the particle sizes of as-received powders.

Secondly, following the optimization of milling frequency, further variations of BPR were also undertaken to enhance the integration, while delivering a handful amount of powder for PCM preparation. As shown in Figure 5(a), the rise in BPR gradually flattens the volume distribution of lower peaks which in turn heightens the desired singular peak at a fair SiC@AlN particle size falling between the average sizes for as-received AlN and SiC powders. Given 20 : 1 as BPR, 0.3301 g of powder was prepared in a single run for PCM reinforcement.

Thirdly, following the optimization of milling frequency and BPR, the milling time was studied to conclude the process. Figure 5(b) displays the PSD graphs with respect to changes in the milling time. Results imply the consistency of the average SiC@AlN particle size after 60 min (up to 120 min) maintaining 33.9 μm in value. The only difference was the slight reduction observed in the number of smaller particles. Hence, according to Figures 4 and 5, the optimum milling conditions for obtaining the largest SiC@AlN particles would be 60 minutes of mechanical alloying while milling frequency and BPR are at 50 Hz and 20 : 1, respectively.

3.3. XRD Analysis. X-ray diffraction (XRD MAX-2500, Rigaku Corp., Japan) analysis was carried out to establish a better understanding of the powder integration via ball milling. As seen in Figure 6, the crystal structure of singular ceramic powders was barely altered after low-energy milling. High-energy milled powders, however, have responded well

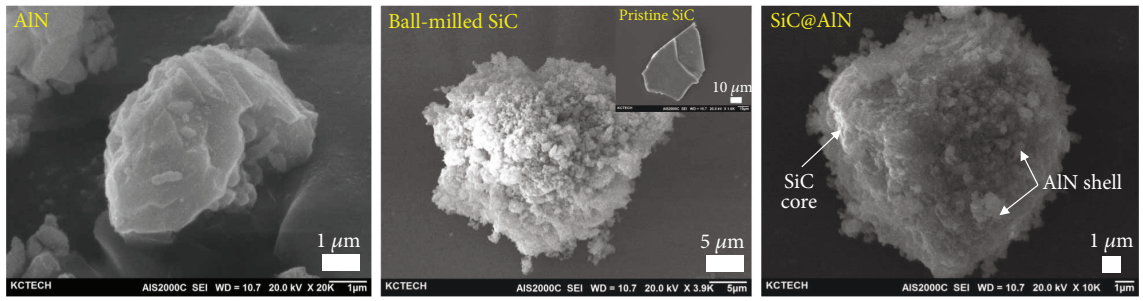

Figure 3: SEM images of the as-received and as-prepared particles.

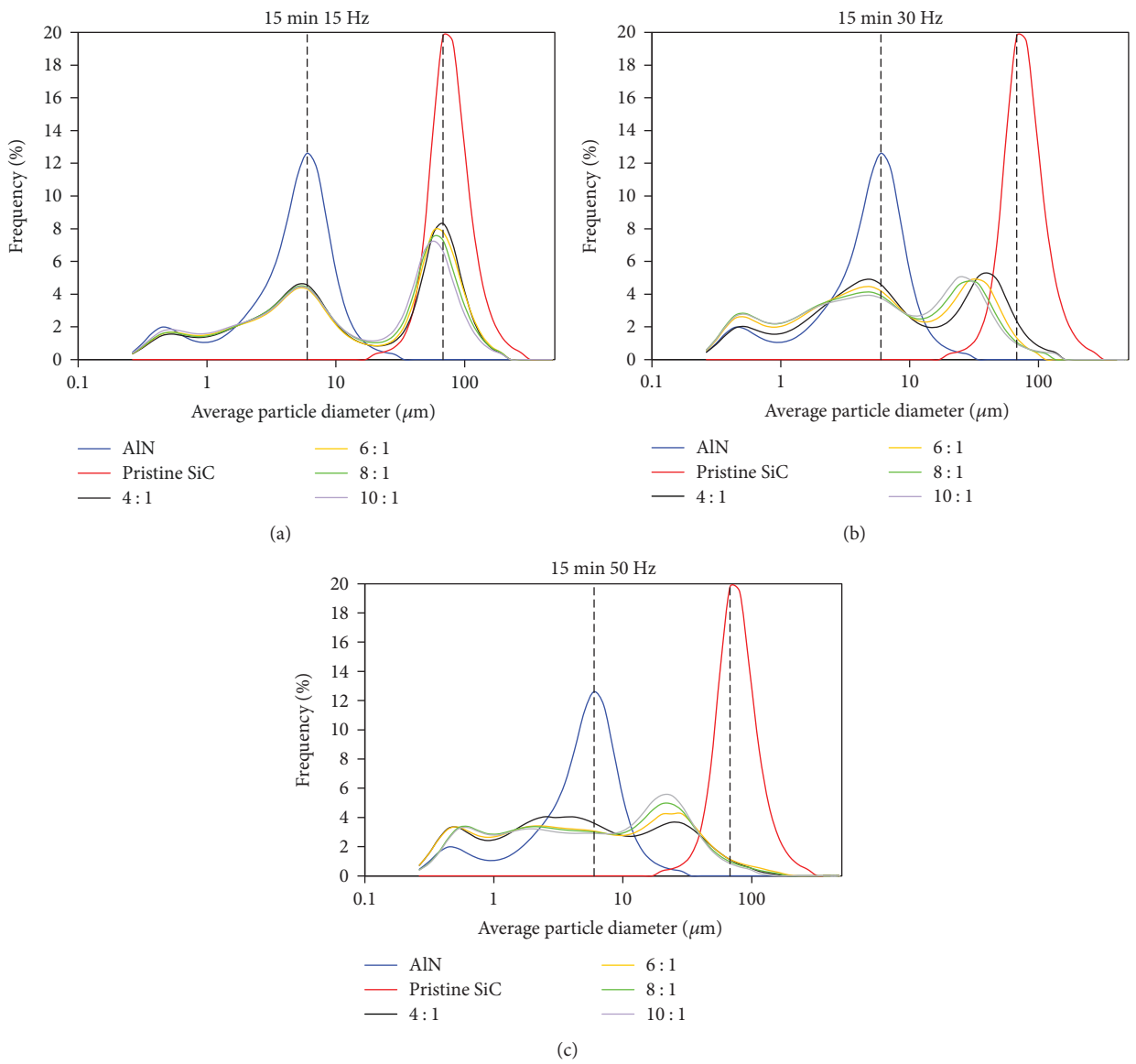

Figure 4: PSD graphs of AlN, pristine SiC, and SiC@AlN (50 wt.% AlN/50 wt.% SiC) powders with respect to different milling frequencies and BPRs.

to lattice integration as the peaks for SiC and AlN are merged at $2\theta = 35.5^{\circ}$, 37.6°, 60°, 65°, and 71°. This can be attributed to the formation of SiC@AlN particles due to mechanical stresses and temperature growth in the vial. Also, the increase in milling time will result in Bragg's angle shift implying exertion of higher levels of uniform strains. XRD

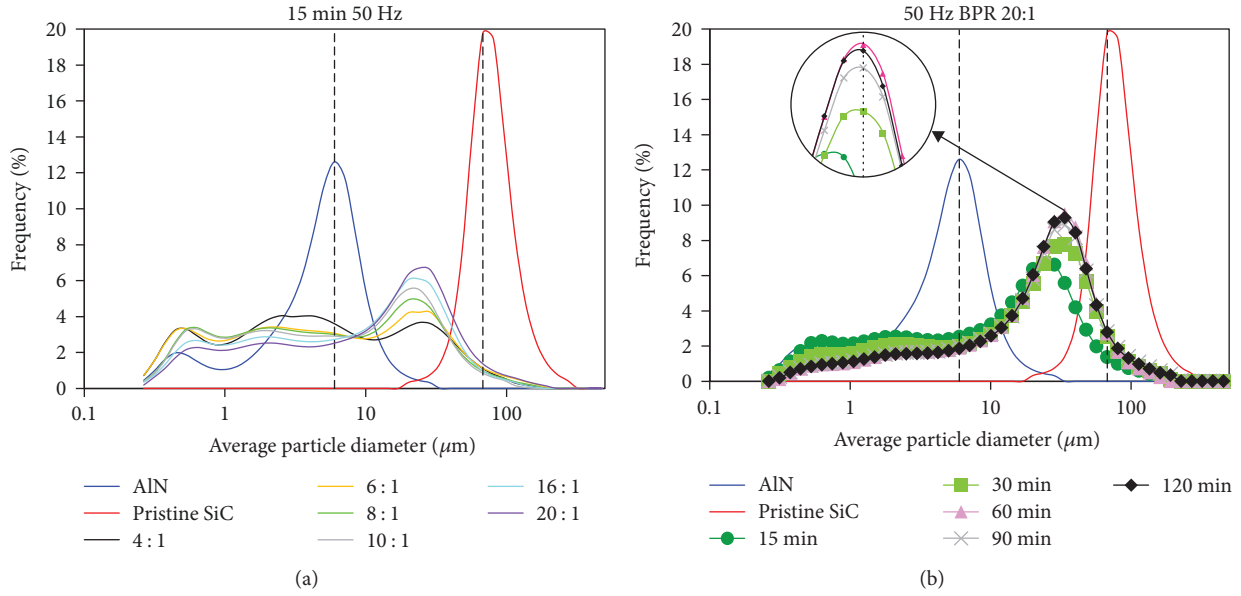

Figure 5: PSD graphs of AlN, pristine SiC, and SiC@AlN (50 wt.% AlN/50 wt.% SiC) powders with respect to different BPRs and milling periods.

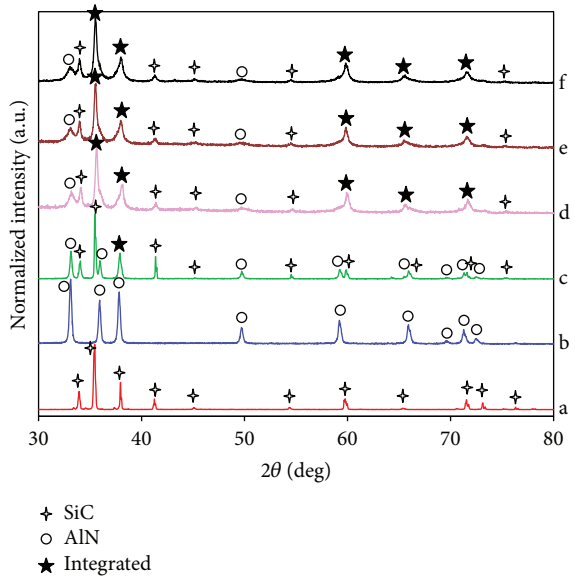

Figure 6: XRD patterns of SiC (a), AlN (b), and SiC@AlN powders after low-energy milling ($t_{BM} = 15$ min, $f_{BM} = 15$ Hz, BPR $\equiv 4:1$) (c) and high-energy milling ($f_{BM} = 50$ Hz, BPR $\equiv 20:1$) where the milling times were 60 (d), 90 (e), and 120 min (f).

then confirms the previous statement claiming that the integration was adequately done by 60 min of milling and a further increase in the time will merely reduce the number of smaller particles.

3.4. Surface Properties. The surface free energy (SFE) of reinforcing powders was analyzed using the sessile drop technique (Tilt Controller, Surface Electro Optics, Korea). Several samples were prepared using uniformly dispersed powder over adhesive tapes. Distilled water and diiodomethane (Sigma-Aldrich Chemicals Company, United States) were then used as the probe liquids to observe the contact angle for each case of dispersed powder. Measurements were carried out several times to ensure the reliability of contact angle values. Then, to calculate the values of SFE using the obtained average contact angle, the Owens-Wendt theory [24] was employed for the extrapolation of the results through the analysis program (Surfaceware 9, Surface Electro Optics, Korea). As illustrated in Table 2, the SiC powder exhibits greater total SFE compared with AlN and hybrid SiC@AlN particles. The obtained SFE values were then used to calculate the work of adhesion (WA) between the components [25–28]. In thermodynamics, WA is explained as the work required for dividing one surface into two separate surfaces. For composites, this can be defined as the amount of work required to separate the filler from the matrix. Accordingly, a larger value of this surface parameter in a multicomponent system means a greater adhesion between the components (filler and matrix). This parameter is calculated using

$$\mathrm{WA} = 2\sqrt{\sigma_M^D \sigma_F^D} + 2\sqrt{\sigma_M^P \sigma_F^P}, \quad (1)$$

where σ_M and σ_F are the SFE values for matrix and filler materials, respectively. Superscripts D and P stand for dispersive and polar components of the SFE.

The respective results for WA of different PCM composite systems are also shown in Table 2. It can be seen that compared to pristine AlN, WA was slightly improved in PCM reinforced with SiC@AlN, which implies improvement of interfacial adherence between paraffin and the biceramic filler. However, SiC possesses the largest value of WA and it is presumably due to the greater dispersive component of

Table 2: Surface free energy of the reinforcing powders.

Sample	Contact angle (deg)		Surface free energy (mJ/m^2)			WA (mN/m)
	Water	Diiodomethane	Dispersive	Polar	Total	
Paraffin	87.44 (±0.367)	56.08 (±0.825)	32.688	2.363	35.051	—
AlN	84.63 (±2.477)	22.28 (±2.247)	45.797	1.180	46.977	80.722
SiC	14.9 (±1.103)	9.5 (±0.408)	43.310	32.383	75.693	92.747
SiC@AlN	74.18 (±3.207)	13.22 (±0.545)	47.131	3.763	50.894	84.465

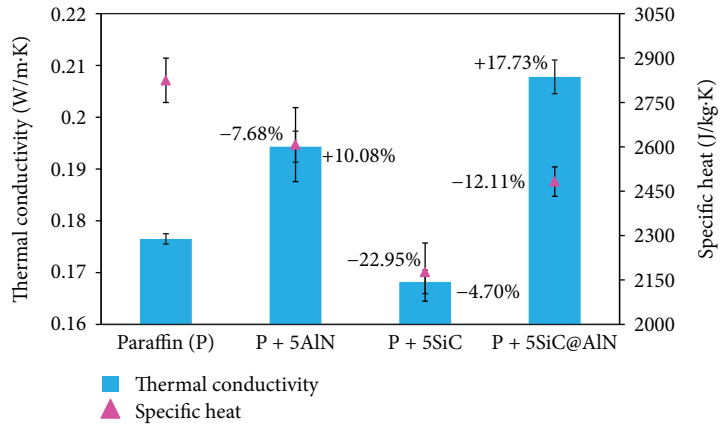

Figure 7: Thermal conductivity and specific heat of fabricated composite PCMs compared with those of pure paraffin. Growth and reduction percentages of parameters against pure paraffin are marked by plus (+) and minus (−) signs, respectively.

SFE of the powder. The SiC powder used for this study has a high Si/C ratio which in turn decreases its polarity and gives the powder a mild viridescent colour.

3.5. Thermal Conductivity. Thermal conductivity (TC) and specific heat (SH) of the samples were measured via a transient plane source method using a Hot Disk instrument (Hot Disk, TPS 2500 S, Hot Disk AB, Sweden). A nickel coil wrapped in Kapton with a diameter of 3.2 mm (#5465) was used as the measuring probe for TC. The estimated data reproducibility and accuracy of the equipment provided by the manufacturer are better than 1% and better than 5%, respectively. The SH value of the fabricated composite PCM was also measured using a highly conductive golden cell as the reference. Results are shown in Figure 7 with the percentages of the change in each parameter compared with that of pure paraffin as the reference. Each sample was measured by more than four times, and the standard deviation bars can also be seen. The standard deviation for TC and SH is less than 2% and less than 5%, respectively.

Addition of AlN powder increases the value of TC by more than 10% compared with that of pure paraffin. SiC powder, however, not only does not improve the energy conduction capability of paraffin but also lessens this value by about 4.7% presumably due to the introduction of crystallite impurities and amorphous phases after ball milling. It is assumed that despite the lower Kapitza resistance between SiC and paraffin (see Section 3.4), phonons are scattered via the SiC lattice defects and grain boundaries. Also, the porous structure of SiC may lead to a larger volume of air voids which in turn reduces the TC. The highest increase in TC was achieved using SiC@AlN biceramic as the filler. This is attributed to the integration of major accommodating characteristics of the two ceramic components resulting in better adsorption of paraffin by the biceramic powder. Also, according to the percolation theory, the percolation threshold of particles decreases by using the mixture of powders with bimodal PSD [29] which in turn increases the chance of formation of longer-range pathways for heat conduction.

This is also evidenced by energy dispersive X-ray spectrometry (EDS, Oxford Instruments, United Kingdom) of composites' cross-sectional area. Samples were linearly notched and submerged under liquid nitrogen for approximately 10 min before the breakage. Figure 8 shows the distribution of elements across the fracture area. It can be easily seen that conductive networks are better formed using the SiC@AlN filler. Comparing all three cases, P + 5SiC@AlN exhibits the larger density of particles across the composite with a higher number of networking bridges, while P + 5AlN falls in the second place pushing the composite reinforced with SiC to the last. This trend properly corresponds to the results obtained for thermal conductivity.

As preceded by the rule of mixture, specific heat of the fabricated blend drops with the use of all types of fillers studied. The largest reduction occurs with SiC as the reinforcing agent. AlN and SiC@AlN on the other hand exhibit better storage capacities of thermal energy in the solid state. Also, this could result from the coarse AlN particles (6 μm) and the larger SiC@AlN particles which are dispersed more uniformly compared with the isotropic scattering of larger SiC particles (28.53 μm).

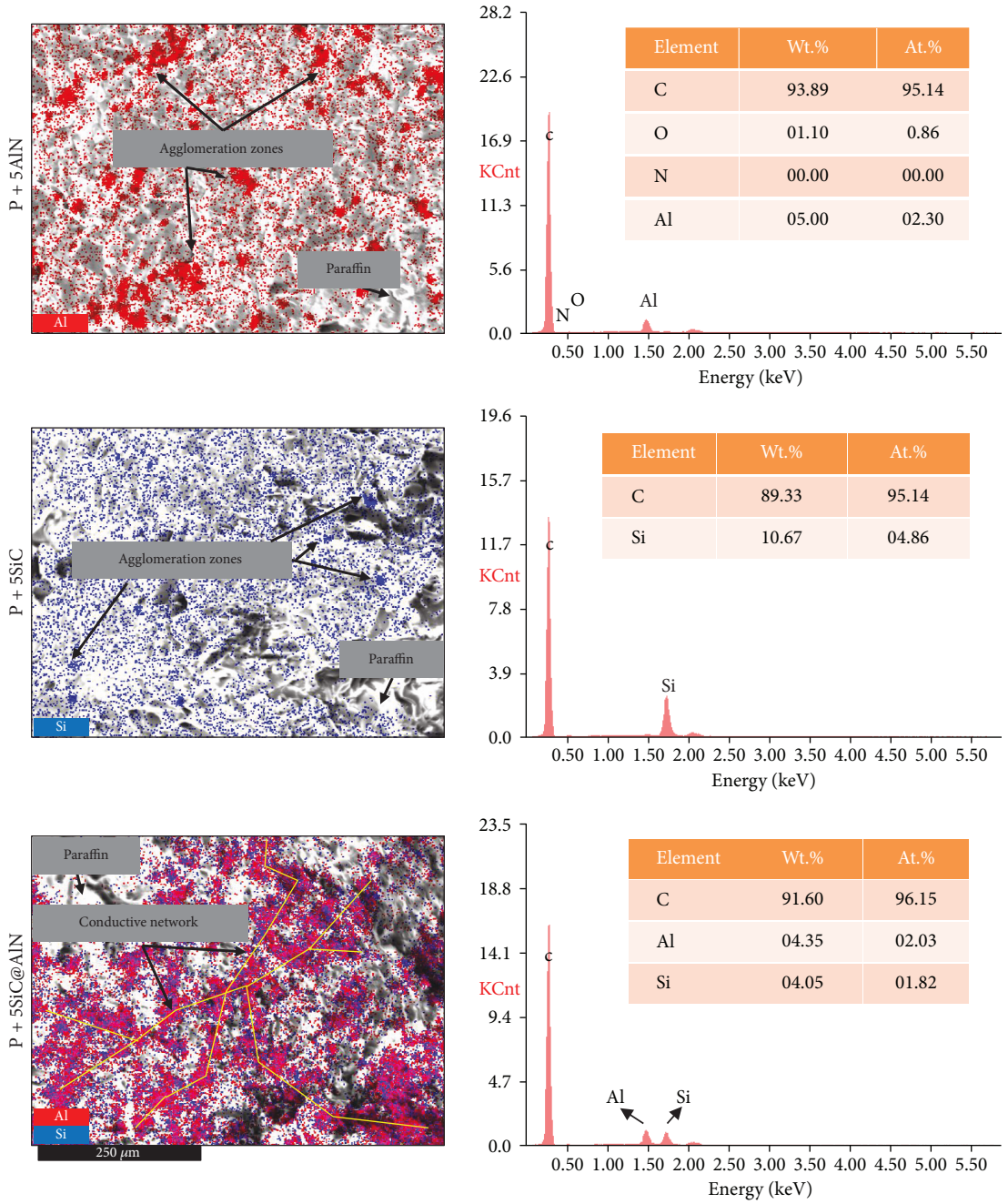

Figure 8: EDS mapping of composite cross sections and their respective elemental compositions.

Figure 9 shows the values of thermal conductivity for P + 5SiC@AlN according to different durations of the mechanical alloying process. As seen here, the biceramic filler after 60 min of milling exhibits the highest conductivity which confirms the optimum condition of ball milling obtained in Section 3.2.

3.6. DSC Thermograms of Fabricated PCMs. The final fabricated material is to be ultimately used as a phase change medium under high charge/discharge rates for energy storage and retrieval. Differential scanning calorimetry (DSC-60, Shimadzu Corp., Japan) was employed to explore the behaviour of the fabricated composite PCM under the variation of temperatures and also to observe the phase change utility of the material by fluctuations in the energy response. A small piece of solidified PCM (7 mg) was placed inside an aluminium hermetic pan (S201-53090, $T_{Max} = 300^{\circ}C$, $P_{Max} = 0.3$ M Pa; Shimadzu Corp., Japan) and then melted to ensure the uniform distribution of the sample in the holder. Prior to measurement, the sample was cooled down to room temperature to minimize the effect of residual heat within the specimen. Following the insertion of the sample and reference into the measurement chamber, experimental parameters including heating rate and the lowest and highest measurement temperatures for both endothermic and exothermic

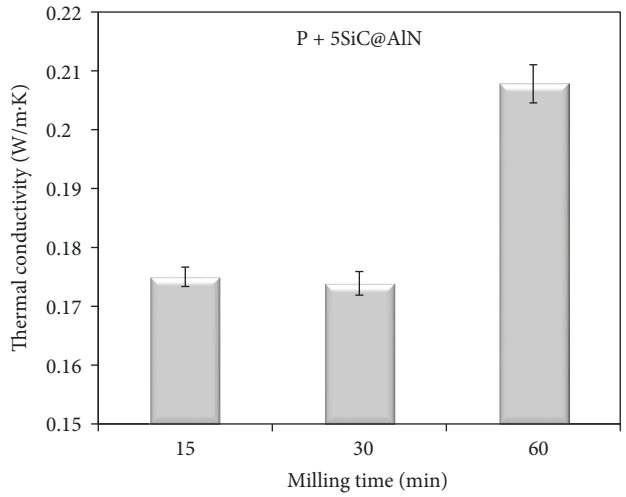

Figure 9: Thermal conductivity of paraffin reinforced with 5 wt.% of SiC@AlN powder as a function of milling time.

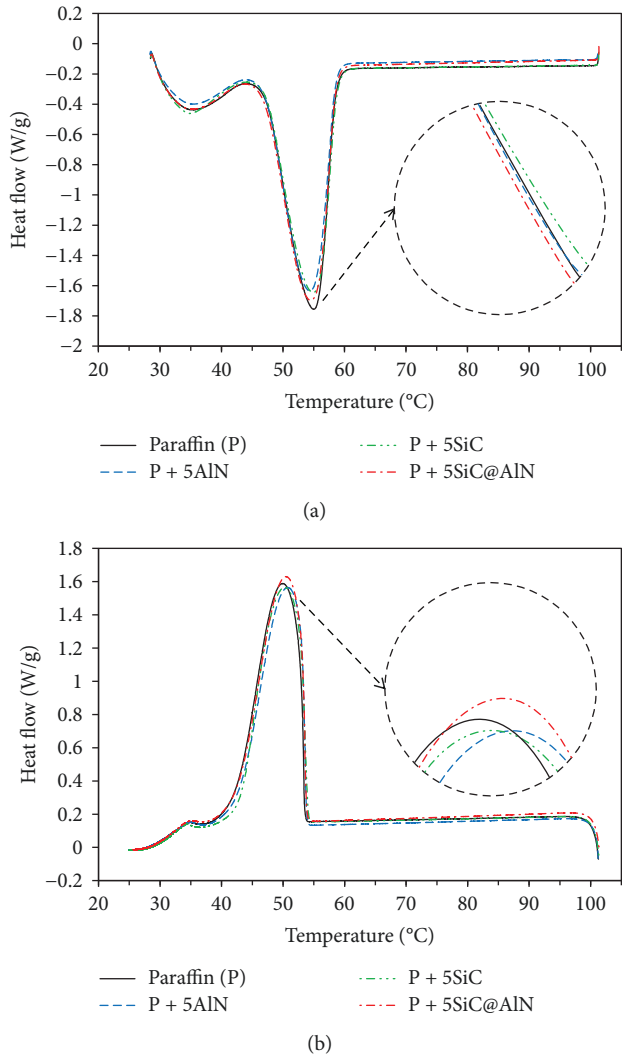

Figure 10: DSC thermograms of (a) endothermic and (b) exothermic runs for the fabricated composite PCMs and pure paraffin.

Table 3: Experimental values of DSC analysis for the fabricated composite PCMs and pure paraffin.

Sample	Run	Phase change temperature (°C)			Latent heat (J/g)
		T_{Onset}	T_P	T_{Endset}	
Paraffin (P)	Endo	47.22	55	58.21	135.02
	Exo	53.45	49.93	42.81	142.68
P + 5AlN	Endo	47.16	54.39	58.14	131.28
	Exo	53.74	50.74	43.01	139.57
P + 5SiC	Endo	48.17	54.89	58.49	130.2
	Exo	53.98	50.26	43.14	140.57
P + 5SiC@AlN	Endo	47.39	54.5	58.61	137.69
	Exo	53.73	50.48	42.87	146.8

Endo: endothermic run; Exo: exothermic run.

runs were set at 5°C/min and 25 and 100°C, respectively. Resultant thermograms are shown in Figure 10. The DSC patterns of analyzed cases were slightly different. Each case was measured several times (at least three times) to ensure the stability of the analysis. The obtained values for transition temperatures and latent heat are presented in Table 3.

As seen in the values obtained by DSC analysis, the addition of fillers delays the starting temperature of the phase transition in both heating and cooling runs. Among these, SiC due to its higher melting point (~2730°C) exhibits a longer hold-up in phase change onset temperatures. This also could be caused by the lower thermal conductivity of the bulk composite PCM reinforced with SiC (see Section 3.5) which postpones the heat distribution and subsequently transition of the crystal structure. Also, the absence of accommodating porous networks in SiC particles will result in poor integration with paraffin leading to less functionality as a stable and uniform PCM. This is evidenced by the lower phase change differential temperature and latent heat of P + 5SiC at the endothermic run. The use of the AlN coarse particles as the reinforcing agent indicates slightly higher latent heat compared with that of P + 5SiC in the heating run that can be attributed to better dispersion of the particles within the paraffin and higher level of integration with the matrix due to a surface integration. Both of singular fillers, however, decrease the intrinsic higher latent heat of paraffin which is opposed by what is desired from a material for a reliable LHTS.

Comparing the values of latent heat, paraffin reinforced with SiC@AlN presents slightly greater latent heat than all the cases including pure paraffin. This is due to the formation of a particulate structure with a larger surface area, which was improved by the mechanical alloying method, and higher volume fraction of well-dispersed ceramic particles for energy storage.

4. Conclusions

The present study analyzes the effects of ceramic and biceramic powders on the thermal properties of paraffin for the potential use as a PCM in thermal energy storage systems. SiC microparticles were successfully coated with AlN powder

using ball milling with optimized conditions. However, the crystalline structure of SiC seemed to have undergone a negative alteration due to the high intensity of the mechanical stresses. Composite PCMs were fabricated via ultrasonication, and thermal analyses of the samples are presented. The highest increase in thermal conductivity was achieved using the SiC@AlN filler compared with singular ceramic powders. EDS results indicate a better capability of the SiC@AlN filler to conduct energy at the solid state of PCM with higher ballistic movements of phonons compared with AlN or SiC powder as the filler. DSC analysis also indicates a very slight growth in the latent heat of paraffin reinforced with SiC@AlN powder. This increase, however, would not be considered a meaningful enhancement for the fabricated PCM. Further improvement of LHTS must be pursued using the combination of such materials and surface engineering with the enhancement of the paraffin-filler interface as the main objective.

Lastly, according to Sigma-Aldrich catalogues, SiC (Lot #378097; 250 g: 47.90 USD) costs approximately 4.54 times lower than AlN powder (Lot #241903; 250 g: 217.50 USD) [18]. Therefore, production of such a hybrid filler, according to obtained results, not only improves the properties of the final PCM composite but also economically justifies the addition of SiC as a low-cost extender to the AlN powder.

Data Availability

The raw data used to support the findings of this study are available from the corresponding author upon request.

Conflicts of Interest

The authors declare that they have no conflicts of interest.

Acknowledgments

This research was funded by the National Research Foundation (NRF) of Korea (Grant nos. 2015R1A2A2A01005693 and 2015M3A7B4049716) supported by the Ministry of Science, ICT and Future Planning (MSIP), Korea, and by the Korea Institute of Energy Technology Evaluation and Planning (KETEP) (Grant no. 20152020001240) supported by the Ministry of Trade, Industry & Energy (MOTIE), Korea.

References

[1] K. Chintakrinda, R. D. Weinstein, and A. S. Fleischer, "A direct comparison of three different material enhancement methods on the transient thermal response of paraffin phase change material exposed to high heat fluxes," *International Journal of Thermal Sciences*, vol. 50, no. 9, pp. 1639–1647, 2011.

[2] S. Y. Wu, H. Wang, S. Xiao, and D. S. Zhu, "An investigation of melting/freezing characteristics of nanoparticle-enhanced phase change materials," *Journal of Thermal Analysis and Calorimetry*, vol. 110, no. 3, pp. 1127–1131, 2012.

[3] F. Colella, A. Sciacovelli, and V. Verda, "Numerical analysis of a medium scale latent energy storage unit for district heating systems," *Energy*, vol. 45, no. 1, pp. 397–406, 2012.

[4] Y. Cui, C. Liu, S. Hu, and X. Yu, "The experimental exploration of carbon nanofiber and carbon nanotube additives on thermal behavior of phase change materials," *Solar Energy Materials and Solar Cells*, vol. 95, no. 4, pp. 1208–1212, 2011.

[5] S. S. Sebti, M. Mastiani, H. Mirzaei, A. Dadvand, S. Kashani, and S. A. Hosseini, "Numerical study of the melting of nano-enhanced phase change material in a square cavity," *Journal of Zhejiang University SCIENCE A*, vol. 14, no. 5, pp. 307–316, 2013.

[6] L. Xia, P. Zhang, and R. Z. Wang, "Preparation and thermal characterization of expanded graphite/paraffin composite phase change material," *Carbon*, vol. 48, no. 9, pp. 2538–2548, 2010.

[7] E.-B. S. Mettawee and G. M. R. Assassa, "Thermal conductivity enhancement in a latent heat storage system," *Solar Energy*, vol. 81, no. 7, pp. 839–845, 2007.

[8] N. S. Dhaidan, J. M. Khodadadi, T. A. Al-Hattab, and S. M. Al-Mashat, "Experimental and numerical investigation of melting of phase change material/nanoparticle suspensions in a square container subjected to a constant heat flux," *International Journal of Heat and Mass Transfer*, vol. 66, pp. 672–683, 2013.

[9] C. J. Ho and J. Y. Gao, "Preparation and thermophysical properties of nanoparticle-in-paraffin emulsion as phase change material," *International Communications in Heat and Mass Transfer*, vol. 36, no. 5, pp. 467–470, 2009.

[10] A. Valan Arasu, A. P. Sasmito, and A. S. Mujumdar, "Thermal performance enhancement of paraffin wax with Al_2O_3 and CuO nanoparticles – a numerical study," *Frontiers in Heat and Mass Transfer*, vol. 2, no. 4, 2011.

[11] T.-P. Teng and C.-C. Yu, "Characteristics of phase-change materials containing oxide nano-additives for thermal storage," *Nanoscale Research Letters*, vol. 7, no. 1, p. 611, 2012.

[12] A. Badakhsh, C. W. Park, and B.-J. Kim, "Preparation and analysis of paraffin-based phase change material using aluminum nitride as the reinforcing agent," in *4th International Conference on Nanotechnology, Nanomaterials & Thin Films for Energy Applications*, pp. 70–72, One Central Press, University of Aalto, Finland, 2017.

[13] Y.-L. Cho, J.-w. Lee, C. Park, Y.-i. Song, and S.-J. Suh, "Study of complex electrodeposited thin film with multi-layer graphene-coated metal nanoparticles," *Carbon Letters*, vol. 21, pp. 68–73, 2017.

[14] W.-K. Choi, B.-J. Kim, and S.-J. Park, "Fiber surface and electrical conductivity of electroless Ni-plated PET ultra-fine fibers," *Carbon letters*, vol. 14, no. 4, pp. 243–246, 2013.

[15] W.-K. Choi, H.-I. Kim, S.-J. Kang, Y. S. Lee, J. H. Han, and B.-J. Kim, "Mechanical interfacial adhesion of carbon fibers-reinforced polarized-polypropylene matrix composites: effects of silane coupling agents," *Carbon letters*, vol. 17, no. 1, pp. 79–84, 2016.

[16] D.-K. Kim, K.-H. An, Y. H. Bang, L.-K. Kwac, S.-Y. Oh, and B.-J. Kim, "Effects of electrochemical oxidation of carbon fibers on interfacial shear strength using a micro-bond method," *Carbon letters*, vol. 19, pp. 32–39, 2016.

[17] A. Badakhsh and C. W. Park, "From morphology of attrited copper/MWCNT hybrid fillers to thermal and mechanical characteristics of their respective polymer-matrix composites: an analytical and experimental study," *Journal of Applied Polymer Science*, vol. 134, no. 41, article 45397, 2017.

[18] Sigma-Aldrich Inc, "Sigma-Aldrich catalog," http://sigmaaldrich.com.

[19] C. X. Guo, X. L. Ma, and L. Yang, "PCM/ graphite foam composite for thermal energy storage device," *IOP Conference Series: Materials Science and Engineering*, vol. 87, no. 1, article 012014, 2015.

[20] Specific Heat Capacity, *Diracdelta.co.uk Science and Engineering Encyclopedia*, Dirac Delta Consultants Ltd, Warwick, England, 2013.

[21] D. D. L. Chung, "Materials for thermal conduction," *Applied Thermal Engineering*, vol. 21, no. 16, pp. 1593–1605, 2001.

[22] J. F. Shackelford and W. Alexander, *CRC Materials Science and Engineering Handbook*, CRC Press, Boca Raton, FL, USA, 3rd edition, 2000.

[23] Y. S. Touloukian, *Thermophysical Properties of High Temperature Solid Materials*, vol. 5, Part 1, 1967, MacMillan Co., New York, United States, 1967.

[24] D. K. Owens and R. C. Wendt, "Estimation of the surface free energy of polymers," *Journal of Applied Polymer Science*, vol. 13, no. 8, pp. 1741–1747, 1969.

[25] O. Sproesser, P. R. Schmidlin, J. Uhrenbacher, M. Eichberger, M. Roos, and B. Stawarczyk, "Work of adhesion between resin composite cements and PEEK as a function of etching duration with sulfuric acid and its correlation with bond strength values," *International Journal of Adhesion and Adhesives*, vol. 54, pp. 184–190, 2014.

[26] S.-J. Park and B.-J. Kim, "Roles of acidic functional groups of carbon fiber surfaces in enhancing interfacial adhesion behavior," *Materials Science and Engineering: A*, vol. 408, no. 1-2, pp. 269–273, 2005.

[27] S.-J. Park, B.-J. Kim, D.-I. Seo, K.-Y. Rhee, and Y.-Y. Lyu, "Effects of a silane treatment on the mechanical interfacial properties of montmorillonite/epoxy nanocomposites," *Materials Science and Engineering: A*, vol. 526, no. 1-2, pp. 74–78, 2009.

[28] K. Jha, E. Anim-Danso, S. Bekele, G. Eason, and M. Tsige, "On modulating interfacial structure towards improved anti-icing performance," *Coatings*, vol. 6, no. 1, p. 3, 2016.

[29] A. Y. Dovzhenko and P. V. Zhirkov, "The effect of particle size distribution on the formation of percolation clusters," *Physics Letters A*, vol. 204, no. 3-4, pp. 247–250, 1995.